Ceramics International 45 (2019) 23917–23923

Contents lists available at ScienceDirect

Ceramics International

journal homepage: www.elsevier.com/locate/ceramint

A new strategy to obtain nano-scale particles of lithium titanate ($Li_4Ti_5O_{12}$) by the oxidant peroxo method (OPM)

Lucas S. Ribeiro[a], André E. Nogueira[c], José M. Aquino[b], Emerson R. Camargo[a,*]

[a] Interdisciplinary Laboratory of Electrochemistry and Ceramics (LIEC), Departament of Chemistry, UFSCar-Federal University of São Carlos, Rod.Washington Luis km 235, CP 676, São Carlos, SP, 13565-905, Brazil

[b] Department of Chemistry, Federal University of São Carlos, C.P. 676, 13560-970, São Carlos, SP, Brazil

[c] Department of Chemistry, Institute of Exact and Biological Sciences (ICEB), Federal University of Ouro Preto-UFOP, Zip Code 35400-000, Ouro Preto, Minas Gerais, Brazil

ARTICLE INFO

Keywords:
Lithium titanate
Ceramics
Peroxo-complexes
Solid state-reaction

ABSTRACT

Lithium titanate with spinel structure ($Li_4Ti_5O_{12}$) has attracted attention for its potential use as anode in lithium-ion batteries. Usually, this material is obtained by solid-state reaction using high temperatures and considerable time in the calcination. Lithium titanate was synthesized in this study using a new approach of the oxidant peroxo method (OPM). The pure spinel phase was obtained by solid-state reaction utilizing commercial LiOH and TiO_2 nanoparticles with surface modified with peroxo-groups (TiO_2-OPM). These nanoparticles were synthesized from the peroxo-complex of titanium, formed on the OPM route. The results show that the use of TiO_2-OPM as precursor favored the production of $Li_4Ti_5O_{12}$ at lower temperature and time when compared to commercial titanium dioxide (TiO_2-COM). The greater reactivity of this powder is related to the peroxo-groups present on the surface of the TiO_2, since their decomposition generates a great amount of energy that accelerates the reaction.

1. Introduction

The technological progress of our society depends on the development and intense use of synthetic materials resulting in a large volume of chemical residues, high-energy consumption and air pollution [1-3]. One of the more efficient ways to reduce carbon dioxide emission and improve air quality in big cities is the use of lithium-ion batteries in electric vehicles and energy storage. In this context, lithium titanate with spinel phase ($Li_4T_5O_{12}$ - LTO) has drawn attention as a potential anode for rechargeable lithium-ion batteries [4-8]. LTO has been obtained by different synthetic methods, such as sol-gel [9-11] or combustion methods [12,13]. Nevertheless, these techniques require expensive reactants and complex procedures. Solid-state reaction (SSR), on the other hand, is simpler, faster and produces larger amount of products per batch [14]. Recently, we combined the conventional SSR with the oxidant peroxo method (OPM) to obtain bismuth titanate of high quality at low temperatures [15]. The OPM route is a new wet-chemical route of synthesis, i.e., uses water as solvent and employs hydrogen peroxide to obtain highly reactive TiO_2 nanoparticles used as precursor in the synthesis of bismuth titanate by solid-state reaction.

The OPM route brought the possibility of obtaining nanometric ceramic powder of technological and commercial interest free of contaminants as carbon and halides [16,17]. Other advantages are the use of water as solvent, low temperature of processing to crystallize nanometric oxides and the absence of toxic subproducts. This technique has successfully yielded important technological materials based on lead and bismuth using titanium and zirconium, i.e. lead titanate, lead zirconate titanate and bismuth titanate [17-27]. All materials were synthesized using lower temperatures than the ones previously reported with no secondary phase, showing the high reactivity of the route.

In this study, we present a new approach of the OPM route to obtain nano-scale particles of lithium titanate with spinel structure. LTO was synthesized by solid-state reaction, employing reactive titanium dioxide nanoparticles with surface modified with peroxo-groups obtained from the OPM route. These nanoparticles were used in order to reduce the temperature and calcination time. Thus, the reactivity of the modified powders of titanium dioxide was compared to the reactivity of two other precursors: a control material (TiO_2-RED) with the surface free from peroxo groups, and commercial titanium dioxide (TiO_2-COM). In addition, a study of the best conditions (time and temperature of calcination) to obtain pure LTO was carried out.

* Corresponding author.
E-mail address: camargo@ufscar.br (E.R. Camargo).

https://doi.org/10.1016/j.ceramint.2019.07.274
Received 16 May 2019; Received in revised form 4 July 2019; Accepted 23 July 2019
Available online 24 July 2019

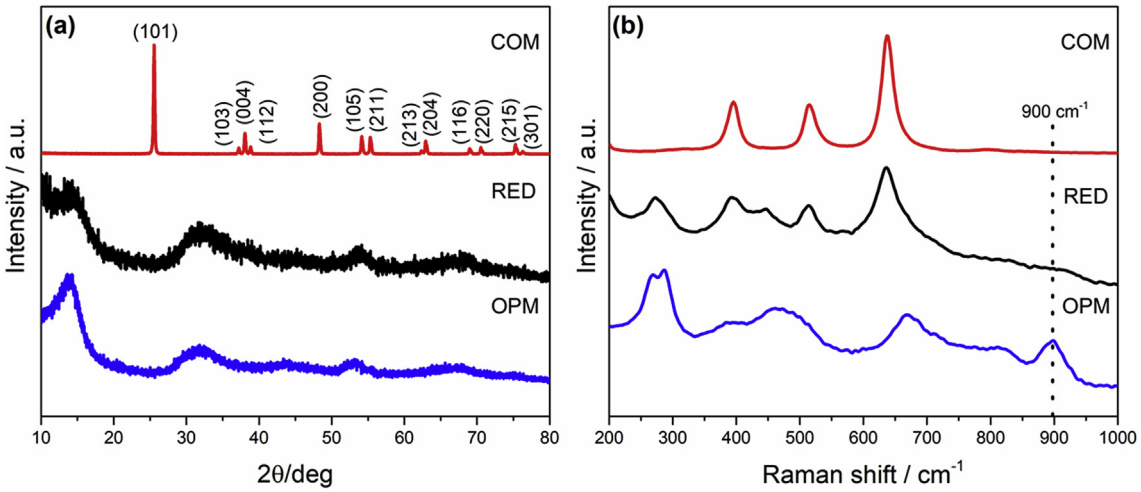

Fig. 1. XRD patterns (a) and Raman spectra (b) of titanium dioxide.

2. Materials and methods

2.1. Synthesis of reactive titanium dioxide

The titanium dioxide with modified surface with peroxo groups was synthesized using a titanium peroxo-complex. In this synthesis, 1 g of titanium metal (LoAH 99%) was added in 300 mL of a solution 3:2H_2O_2 (Synth 30%) and NH_3 (Synth 27%) under ice bath until the metal was completely dissolved (approximately 12 h), which resulted in a transparent yellow solution (titanium peroxo-complex). This complex was heated at 80 °C under constant stirring until a yellow gel was formed. The gel was dried at 60 °C to obtain the yellow powder of TiO_2 with modified surface that was denominated TiO_2-OPM. A control sample was produced through a treatment by heating TiO_2-OPM at 250 °C for 30 min under H_2 flux that was denominated TiO_2-RED.

2.2. Synthesis of lithium titanate

LiOH (Sigma Aldrich 98%), commercial TiO_2 (Merck 99%, TiO_2-Com), and the as-prepared TiO_2-OPM and TiO_2-RED were used to produce lithium titanate with spinel phase structure ($Li_4Ti_5O_{12}$) by a solid-state reaction. Stoichiometric quantities of lithium hydroxide and titanium dioxide with 4:5 M ratio were mixed in a ball-mill for 24 h using zirconia spheres with 3 mm of diameter and isopropanol (Synth 99%) as milling media. The mixture was dried at 60 °C for 24 h and calcined at different temperatures (650, 700, 750, 850 °C) for 0.5, 1, 2 and 3 h.

2.3. Characterization

All powders were characterized at room temperature by X-ray diffraction (XRD) using Cu Kα radiation (Rikagu D/Max 200 with a rotary anode operating at 150 kV and 40 mA) in the 2θ range from 10° to 80°, with a step scan of 0.02°. Raman spectra were obtained with a Horiba Jobin-Yvon Raman micro-spectrometer LabRAM at room temperature using the 633 nm line of a 5.9 mW He–Ne laser as the excitation source through an Olympus TM BX41 microscope. The morphology of the powder was characterized by scanning electron microscopy (SEM-FEG, ZEISS model-SUPRA 35). Chemical surface analyses were performed on a K-Alpha XPS (Thermo Fisher Scientific, UK) using Al Kα X-rays, vacuum > 10-8 mbar and charge compensation during measurements. A resolution of 1 eV with 5 scans was used for the survey spectra whereas the high-resolution spectra were recorded with resolution of 0.1 eV and 50 scans. The binding energy was referenced to the C 1s peak at 284.8 eV. Data analysis was performed using the CasaXPS software. Thermal analysis were carried out using an a TGA Q500 thermogravimetric analyzer (TA Instruments, New Castle, DE), in air flow and recorder from room temperature to 400 °C, with a heating rate of 10 °C/min and the TiO_2-OPM was characterized by differential scanning calorimetry (DSC 404C controlled by TASC 424/3A, Netzsch, Germany) between 50 and 400 °C using an aluminum crucible and a constant heating/cooling rate of 10 °C/min with a flux of 0.50 cm^3/min.

3. Results and discussion

The OPM route was developed for the synthesis of lead-based compounds. This route is based on the exothermic reaction between water soluble Pb^{2+} and H_2O_2 at high pH [16,17]. In low pH, the Pb(II) solution is stable in the presence of hydrogen peroxide, but at high pH a highly exothermic reaction occurs. Thus the main idea of OPM route is the substitution of H_2O_2 by a soluble inorganic peroxo-complex in water, which react with Pb(II) in a similar way oxidizing to Pb(IV) [17]. In this reaction the complex is hydrolyzed into TiO_2 as shown by Equation (1):

$$Pb(OH)_{4(aq)}^{2-} + [Ti(OH)_3O_2]^-_{(aq)} \rightarrow PbO_{2\ (s)} + TiO_{2\ (s)} + 2H_2O_{(l)} + 3OH^-_{(aq)} \quad (1)$$

Therefore, TiO_2-OPM was obtained using the same principles of peroxo-complex hydrolysis through the formation of water by the oxidation of H_2O_2. But, instead of the redox reaction, the solution was heated making the hydrogen peroxide decomposes forming O_2 and H_2O, resulting in titanium dioxide with the surface modified with peroxo groups (TiO_2-OPM) [15]. The TiO_2-OPM powder showed a yellow coloration that is related to the presence of the peroxo-groups on the TiO_2 surface as reported in previous work of the group [15]. The control precursor (TiO_2-RED) was produced applying H_2 flux in TiO_2-OPM powder to remove the peroxo-groups and showed a white coloration, preserving the crystalline structure of nanoparticles as well its particle size distribution.

Fig. 1 shows the XRD patterns and Raman spectra of the powders of TiO_2-OPM, TiO_2-RED and TiO_2-COM. Fig. 1a shows that both precursors obtained by the OPM route, TiO_2-OPM and TiO_2-RED, have no long range order, which is characterized by the lack of strong peaks in the diffractograms. However, Raman spectra in Fig. 1b shows that these materials have bands that can be related to the anatase phase, being more pronounced in the TiO_2-RED spectrum. Another important fact is that the white powder of TiO_2-RED presented the same XRD pattern of TiO_2-OPM, which indicates that its structure, and particle size were preserved after the treatment to remove part of the peroxo-groups bond to the surface. This result shows that the only difference between TiO_2-

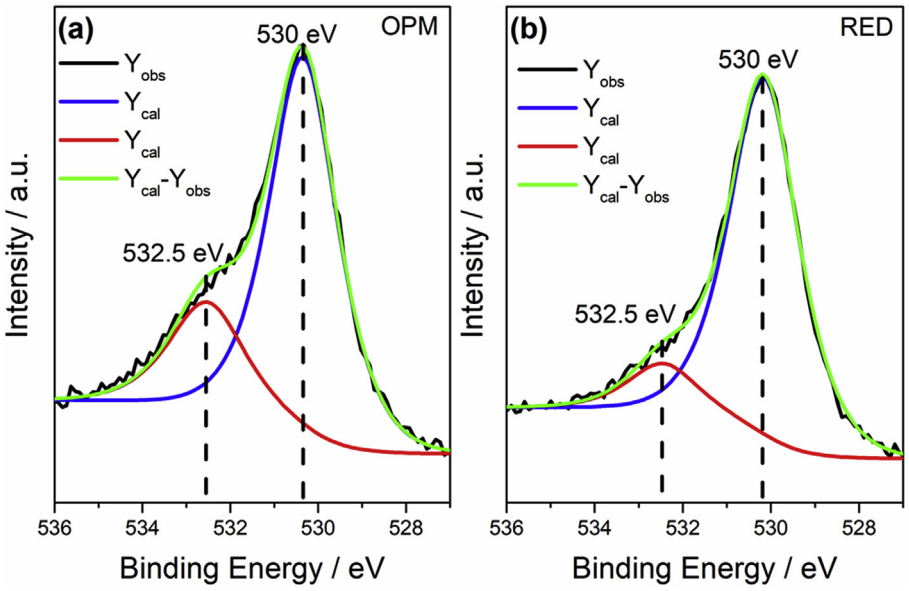

Fig. 2. X-ray photoelectron spectroscopy (XPS) spectra of O1s for (a) TiO_2-OPM and (b) TiO_2-RED. (For interpretation of the references to color in this figure legend, the reader is referred to the Web version of this article.)

OPM and TiO_2-RED is the amount of peroxo-groups in the surface.

Raman spectra of these powders are shown in Fig. 1b. The TiO_2-OPM spectrum shows a band in the region 880-940 cm^{-1} related to the O-O stretching vibration. This same result for peroxo-groups on the surface of titanium dioxide was reported by Zou et al., confirming the modification on the surface of these nanoparticles [28]. However, the same band cannot be observed in the spectrum of the TiO_2-RED, which confirms the partial removal of peroxo groups in the surface. As expected, the TiO_2-COM powder presented a spectrum related to the anatase crystalline phase [29].

Francatto et al. reported that XPS spectra of powders of TiO_2-OPM and TiO_2-RED are different with a decrease in the intensity of a peak with binding energy of 531 eV, which is related to the peroxo-group. The same methodology for the remove of peroxo-groups was used and the result obtained in this study is shown in Fig. 2. The difference to the reported result is that the XPS spectrum of TiO_2-RED showed a shoulder in the region of peroxo-groups that cannot be seen in the XPS spectrum reported by Francatto et al., meaning that even after the treatment, some peroxo-groups were preserved in the surface [15].

The TEM images of TiO_2-OPM and TiO_2-RED (Fig. 3) show the presence of irregular agglomerates of nanoparticles with no defined morphology. However, TiO_2-COM presents spherical particle agglomerates with a mean particle size of 175 nm.

One of the hypotheses that explain the high reactivity of the powders synthesized by the OPM route is related to the presence of the peroxo-groups in the surface of the amorphous titanium dioxide formed during the synthesis process. Thus, the reactivity of TiO_2-OPM was evaluated by solid-state reaction to obtain $Li_4Ti_5O_{12}$.

Fig. 4a shows the XRD patterns after the TiO_2 precursors reacted with lithium hydroxide at 850 °C for 30 min. The pure spinel phase, with cubic structure (PDF 49-207), was obtained in the synthesis using TiO_2-OPM. The other precursors when calcined at this temperature couldn't react all the TiO_2 present in the mixture. The confirmation is the peak related to the rutile phase marked with a closed circle in the XRD pattern and in the Raman spectrum. The TiO_2-RED presented a small peak in this region, while the TiO_2-COM presented an intense peak.

The powders crystalline structure was also characterized by Raman spectroscopy as can be seen in Fig. 4b. There are five bands active related to lithium titanate with the spinel phase (A_{1g} + E_g + $3F_{2g}$) [14,30-34]. The peak located at 675 cm^{-1} (A_{1g}) with a shoulder at 748 cm^{-1} is originated from the vibrational stretch of the Ti-O covalent bond in the octahedron TiO_6 [30,31,33,34]. The second high-intensity peak at 424 cm^{-1} is related to the vibrational mode of Li-O ion bond stretching located in the LiO_4 (E_g) tetrahedron [31,34]. Three peaks (F_{2g}) located at 353 cm^{-1}, 276 cm^{-1} and 235 cm^{-1} are usually related to the displacement of the oxygen atom, but may also be the movement of lithium ions [32,33]. These results were found for powders calcined at

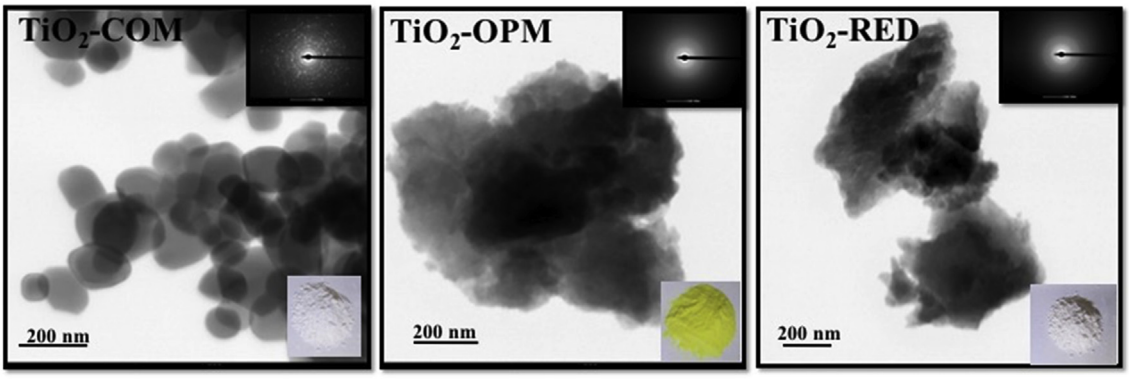

Fig. 3. TEM images of the precursors of titanium dioxide and inset their respective diffractions and photographs.

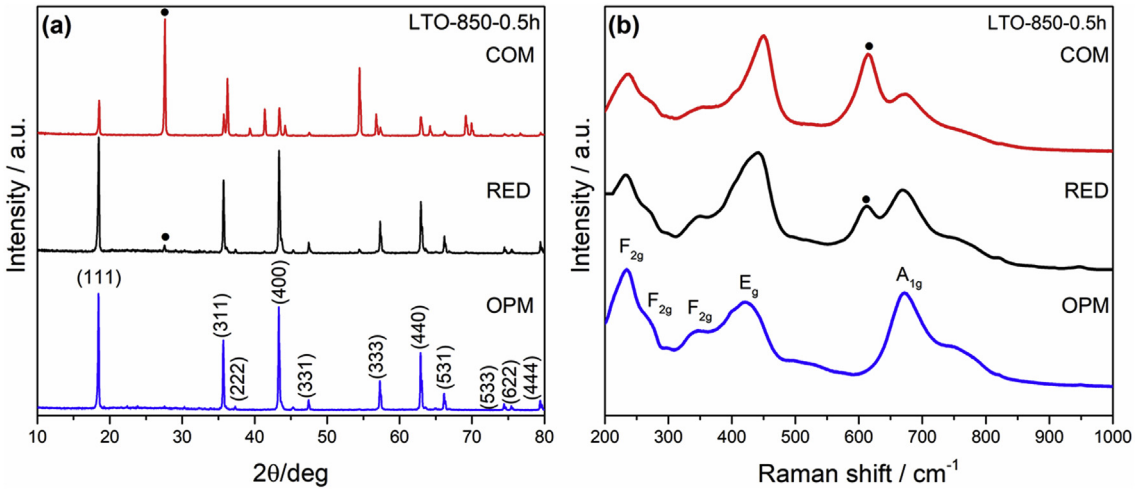

Fig. 4. XRD patterns (a) and Raman spectra (b) of materials synthesized with TiO_2-OPM, TiO_2-RED and TiO_2-COM. (For interpretation of the references to color in this figure legend, the reader is referred to the Web version of this article.)

850 °C when synthesized using TiO_2-OPM. For powders made from TiO_2-RED and TiO_2-COM, the same bands are present, however at 617 cm^{-1} is possible to see a band related to the titanium dioxide with rutile structure, confirming that not all TiO_2 precursor reacted.

The difference in reactivity between these powders can be explained by the number of peroxo-groups in the surface of each precursor. To quantify these groups, the thermogravimetric analysis (TGA) was used. As can be seen in the thermogravimetric curves in Fig. 5, the yellow powder TiO_2-OPM presented 20% of weight loss related to the peroxo-groups between 150-270 °C, while the white powder TiO_2-RED presented 6% of weight loss between 240-270 °C. Since TiO_2-RED powders have reminiscent peroxo-groups, this explains why its reactivity was greater than the commercial titanium dioxide.

The two precursors (TiO_2-OPM and TiO_2-RED) obtained by the OPM route were used to produce LTO in lower temperatures as shown in Figs. 6 and 7. The lithium titanate with spinel phase was obtained in all calcination conditions using both titanium dioxide precursors. The main difference is in the presence of titanium dioxide remaining after the thermic treatment. When the TiO_2-OPM was used in the reaction at 850 °C and 800 °C for 0.5 h, the formation of LTO occurred without secondary phase as can be seen in the XRD pattern and in the Raman spectrum. However, lithium titanate prepared in the same conditions using TiO_2-RED showed the presence of a secondary phase related to the rutile phase of titanium dioxide. The peaks and bands related to rutile are marked with closed circles. The fact that TiO_2-RED did not react completely at 800 °C for 0.5 h to produce pure LTO, even though it has the same structure and particle size than TiO_2-OPM, shows that the greater reactivity of TiO_2-OPM comes from the peroxo-groups in the surface, not only from its structure. When both precursors were calcined at 750 °C for 0.5 h, the secondary phase that can be seen in the Raman spectra is the anatase phase of unreacted titanium dioxide. The bands related to anatase are marked with asterisks. The fact that the peak at 25° in the XRD pattern, as well as the bands in the Raman spectrum related to anatase, is more pronounced in the material produced using TiO_2-RED may indicate that a greater amount of titanium dioxide could not react. This result shows that the titanium dioxide with surface modified with peroxo-groups has a greater reactivity.

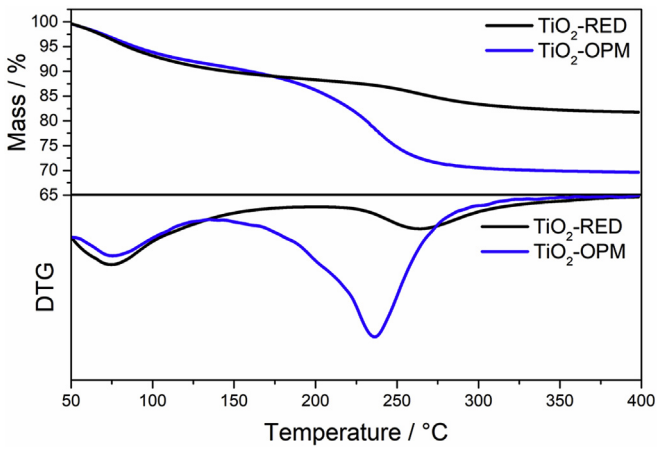

Fig. 5. TGA curve and the first derivative of the TGA curve for TiO_2-OPM (blue) and TiO_2-RED (black). (For interpretation of the references to color in this figure legend, the reader is referred to the Web version of this article.)

The precursor TiO_2-OPM was used to obtain LTO in different conditions at the temperatures of 700, 750, 800 and 850 °C and in the times of 0.5, 1, 2 and 3 h. Fig. 8 shows the diagram with all conditions. As shown in Figs. 6a and 7a, single phase $Li_4Ti_5O_{12}$ was obtained when the amorphous mixtures were calcined at 850 °C and 800 °C for 0.5 h, the lowest time tested. In the diagram these results are represented by black squares in the temperatures of 800 and 850 °C at all times. When the temperature was reduced to 750 °C, the formation of TiO_2-OPM was incomplete, regardless of the calcination time used. The Raman spectra of these powders (Fig. S1) showed bands related to LTO and titanium dioxide. As the calcination time was increased, there was a phase change of titanium dioxide. In the lower times (0.5 and 1 h), the secondary phase was anatase. However, the secondary phase was rutile after 2 h. In Fig. S1 is possible to see the shift of the band at 638 cm^{-1} related to anatase to 612 cm^{-1}, which is related to the rutile phase. These results are represented in the diagram with the shift of blue triangles to red circles in the temperature of 750 °C. When the temperature was further reduced to 700 °C, anatase continued to be present as secondary phase. This result is represented by blue triangles. The Raman spectra of all powders obtained can be seen in Fig. S1 of the supplementary material.

The energy supplied during the calcination showed to be insufficient to consume all the reactants, and the decomposition of peroxo-groups plays an important role in the crystalline structure formation of lithium titanate. The differential scanning calorimetry (DSC) was used to measure the energy released during the decomposition of peroxo-groups in the precursors TiO_2-RED and TiO_2-OPM. The exothermic decomposition of peroxo-groups is in the temperature range of 200–300 °C for both precursors. TiO_2-OPM presented two events, one at 222 °C and a secondary event at 260 °C. TiO_2-RED showed only one event at 274 °C. Fig. 9 shows that the TiO_2-OPM released more energy

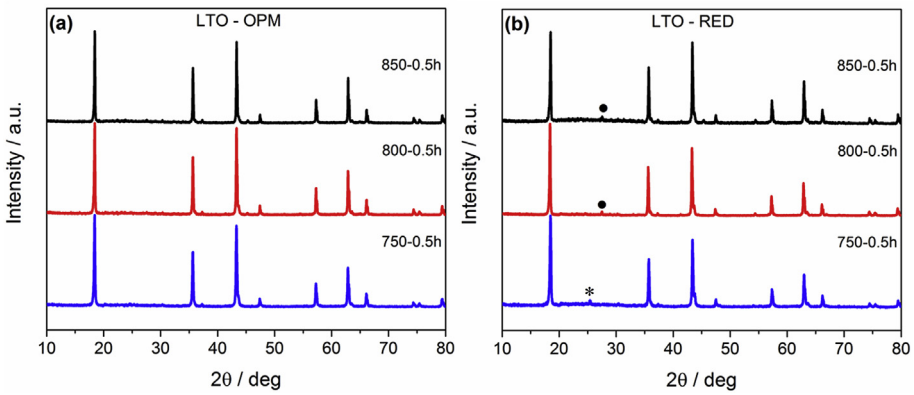

Fig. 6. XRD patterns of materials synthesized with TiO_2-OPM (a) and TiO_2-RED at different temperatures and time. (For interpretation of the references to color in this figure legend, the reader is referred to the Web version of this article.)

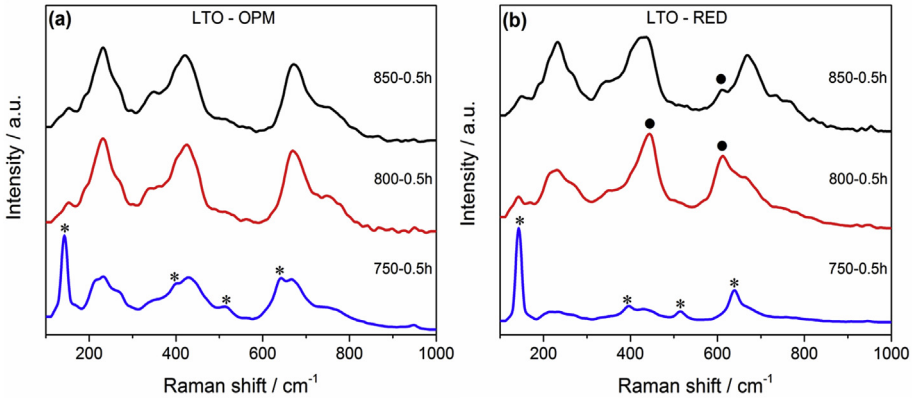

Fig. 7. Raman spectra of materials synthesized with TiO_2-OPM (a) and TiO_2-RED at different temperatures and time. (For interpretation of the references to color in this figure legend, the reader is referred to the Web version of this article.)

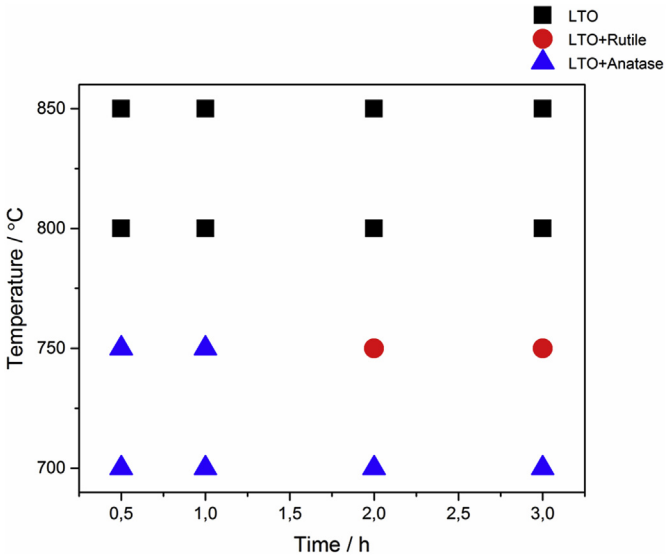

Fig. 8. Diagram with all condition used to calcined the amorphous mixture of titanium and lithium to produce $Li_4Ti_5O_{12}$.

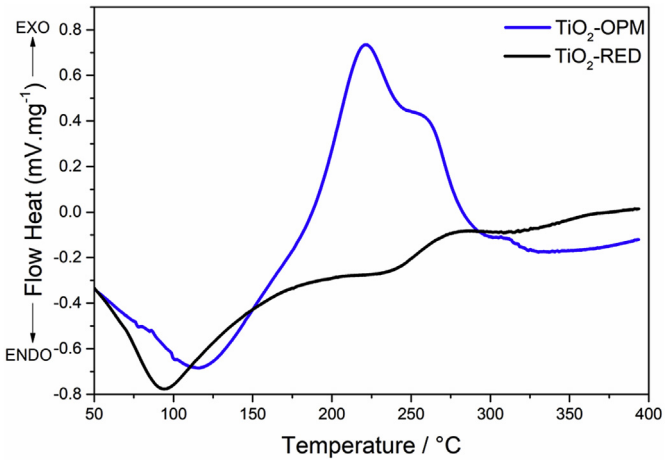

Fig. 9. DSC curve of TiO_2-OPM (blue) and TiO_2-RED (black). (For interpretation of the references to color in this figure legend, the reader is referred to the Web version of this article.)

during the process of loss of peroxo-groups, which is in agreement with the thermogravimetric analysis. Its decomposition released 305 J/g, while TiO_2-RED released 22.2 J/g. This difference is responsible for the higher reactivity of TiO_2-OPM, which is capable of forming LTO at 800 °C for 0.5 h with no secondary phase.

In the case of TiO_2-OPM nanoparticles, the peroxo-groups bond to the surface decompose exothermically [35], which means that they can act as an energy source similar to other reactants used in self-propagating high-temperature synthesis (SHS), which a highly exothermic reaction releases a great amount of energy locally that is used to activate the main process, reducing the necessary temperature and reaction time. A conventional solid-state reaction needs considerable quantity of energy of external source to overcome the kinetic barrier, but a small amount of energy is required to start the decomposition of peroxo-

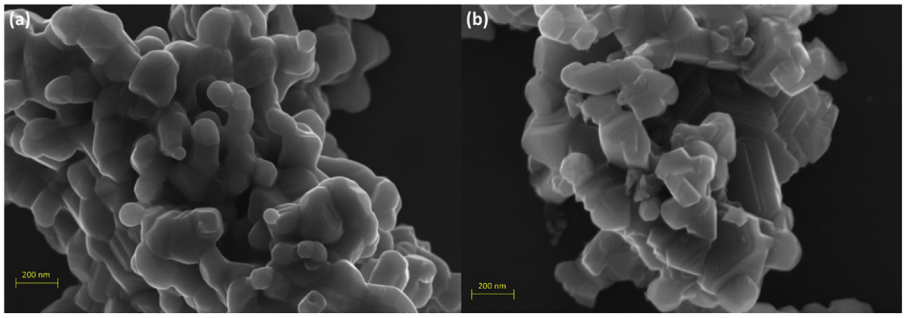

Fig. 10. SEM of LTO synthesized with TiO_2-OPM (a) and TiO_2-RED at 850 °C for 0.5 h. (For interpretation of the references to color in this figure legend, the reader is referred to the Web version of this article.)

groups bond to the surface of reactive TiO_2 [15]. Since a short time is necessary to disperse this released energy, it can be considered a good approximation of an adiabatic transformation, resulting in enough local energy to activate the nanoparticles surface to react faster and at lower temperatures [36].

The synthesis using solid-state reaction to obtain lithium titanate with spinel phase usually employs high temperature and a long period of time in the calcination. Sivashanmugam et al. obtained the same phase by solid-state reaction with the calcination being done at 850 °C for 10 h [37]. Babu et al. synthesized $Li_4Ti_5O_{12}$ calcining the mixture of commercial lithium carbonate and titanium dioxide at 850 °C for 16 h [38]. This new result at 800 °C for 0.5 h shows the great impact that the OPM route can have in obtaining ceramic powders using solid-state reactions.

Scanning electronic microscopy was performed for the samples of LTO synthesized using TiO_2-OPM and TiO_2-RED and calcined at 850 °C for 0.5 h. It is possible to see in Fig. 10 that none of the samples has defined morphology and controlled nanoparticle size. However, the LTO synthesized with titanium dioxide with peroxo-groups showed some coalescent particles due to the high energy released by these groups during the calcination process.

4. Conclusions

The lithium titanate powder was successfully synthesized by the new approach of the OPM route using stoichiometric Li:Ti molar ratio. The calcination temperature of 800 °C and time of 0.5 h was found enough to produce spinel ($Li_4Ti_5O_{12}$) phase powder. The higher reactivity of TiO_2-OPM when compared with TiO_2-COM and TiO_2-RED was confirmed since the other reactants couldn't produce pure LTO in the same conditions of calcination. The peroxo-groups exothermic decomposition generates a great amount of energy that accelerates the reaction. This new approach opened the possibility of synthesizing important technological ceramics through OPM route based in other elements, not only lead and bismuth.

Acknowledgements

The authors would like to thank the financial support given by São Paulo Research Foundation - FAPESP (grants 2015/13958-3, 2014/25616-7, 2016/14667-5, 2014/09014-7, 2018/12871-0), CEPID (2013/07296-2), National Council for Scientific and Technological Development - CNPq and Coordination of Higher Education Personnel - CAPES.

Appendix A. Supplementary data

Supplementary data to this article can be found online at https://doi.org/10.1016/j.ceramint.2019.07.274.

References

[1] K.M. Colbow, J.R. Dahn, R.R. Haering, Structure and electrochemistry of the spinel oxides LiTi2O4 and Li43Ti53O4, J. Power Sources 26 (1989) 397–402.
[2] B. Li, C. Han, Y.-B. He, C. Yang, H. Du, Q.-H. Yang, F. Kang, Facile synthesis of Li4Ti5O12/C composite with super rate performance, Energy Environ. Sci. 5 (2012) 9595–9602.
[3] T. Ohzuku, A. Ueda, N. Yamamoto, Zero-strain insertion material of Li [Li1/3Ti5/3] O 4 for rechargeable lithium cells, J. Electrochem. Soc. 142 (1995) 1431–1435.
[4] G. Jeong, Y.-U. Kim, H. Kim, Y.-J. Kim, H.-J. Sohn, Prospective materials and applications for Li secondary batteries, Energy Environ. Sci. 4 (2011) 1986–2002.
[5] B. Kang, G. Ceder, Battery materials for ultrafast charging and discharging, Nature 458 (2009) 190.
[6] X.-Y. Liu, H.-J. Peng, Q. Zhang, J.-Q. Huang, X.-F. Liu, L. Wang, X. He, W. Zhu, F. Wei, Hierarchical carbon nanotube/carbon black scaffolds as short- and long-range electron pathways with superior Li-ion storage performance, ACS Sustain. Chem. Eng. 2 (2014) 200–206.
[7] A. Wei, W. Li, L. Zhang, B. Ren, X. Bai, Z. Liu, Enhanced electrochemical performance of a LTO/N-doped graphene composite as an anode material for Li-ion batteries, Solid State Ion. 311 (2017) 98–104.
[8] M.S. Whittingham, Lithium batteries and cathode materials, Chem. Rev. 104 (2004) 4271–4302.
[9] G. Yan, H. Fang, H. Zhao, G. Li, Y. Yang, L. Li, Ball milling-assisted sol–gel route to Li4Ti5O12 and its electrochemical properties, J. Alloy. Comp. 470 (2009) 544–547.
[10] T.-F. Yi, L.-J. Jiang, J. Shu, C.-B. Yue, R.-S. Zhu, H.-B. Qiao, Recent development and application of Li4Ti5O12 as anode material of lithium ion battery, J. Phys. Chem. Solids 71 (2010) 1236–1242.
[11] C. Zhang, Y. Zhang, J. Wang, D. Wang, D. He, Y. Xia, Li4Ti5O12 prepared by a modified citric acid sol–gel method for lithium-ion battery, J. Power Sources 236 (2013) 118–125.
[12] J. Wang, H. Zhao, Y. Wen, J. Xie, Q. Xia, T. Zhang, Z. Zeng, X. Du, High performance Li4Ti5O12 material as anode for lithium-ion batteries, Electrochim. Acta 113 (2013) 679–685.
[13] T. Yuan, R. Cai, R. Ran, Y. Zhou, Z. Shao, A mechanism study of synthesis of Li4Ti5O12 from TiO2 anatase, J. Alloy. Comp. 505 (2010) 367–373.
[14] M. Michalska, M. Krajewski, D. Ziolkowska, B. Hamankiewicz, M. Andrzejczuk, L. Lipinska, K.P. Korona, A. Czerwinski, Influence of milling time in solid-state synthesis on structure, morphology and electrochemical properties of Li4Ti5O12 of spinel structure, Powder Technol. 266 (2014) 372–377.
[15] P. Francatto, F.N. Souza Neto, A.E. Nogueira, A.M. Kubo, L.S. Ribeiro, L.P. Gonçalves, L.F. Gorup, E.R. Leite, E.R. Camargo, Enhanced reactivity of peroxo-modified surface of titanium dioxide nanoparticles used to synthesize ultrafine bismuth titanate powders at lower temperatures, Ceram. Int. 42 (2016) 15767–15772.
[16] E.R. Camargo, M.G. Dancini, M. Kakihana, The oxidant peroxo method (OPM) as a new alternative for the synthesis of lead-based and bismuth-based oxides, J. Mater. Res. 29 (2014) 131–138.
[17] E.R. Camargo, M. Kakihana, Peroxide-based route free from halides for the synthesis of lead titanate powder, Chem. Mater. 13 (2001) 1181–1184.
[18] E.R. Camargo, J. Frantti, M. Kakihana, Low-temperature chemical synthesis of lead zirconate titanate (PZT) powders free from halides and organics, J. Mater. Chem. 11 (2001) 1875–1879.
[19] E.R. Camargo, E.R. Leite, E. Longo, Synthesis and characterization of lead zirconate titanate powders obtained by the oxidant peroxo method, J. Alloy. Comp. 469 (2009) 523–528.
[20] E.R. Camargo, M. Popa, J. Frantti, M. Kakihana, Wet-chemical route for the preparation of lead Zirconate: an amorphous carbon- and halide-free precursor synthesized by the hydrogen peroxide based route, Chem. Mater. 13 (2001) 3943–3948.
[21] M.D. Gonçalves, F.L. Souza, E. Longo, E.R. Leite, E.R. Camargo, Dielectric characterization of microwave sintered lead zirconate titanate ceramics, Ceram. Int. 42 (2016) 14423–14430.
[22] A.E. Nogueira, A.R.F. Lima, E. Longo, E.R. Leite, E.R. Camargo, Structure and photocatalytic properties of Nb-doped Bi12TiO20 prepared by the oxidant peroxide method (OPM), J. Nanoparticle Res. 16 (2014) 2653.
[23] A.E. Nogueira, A.R.F. Lima, E. Longo, E.R. Leite, E.R. Camargo, Effect of lanthanum

and lead doping on the microstructure and visible light photocatalysis of bismuth titanate prepared by the oxidant peroxide method (OPM), J. Photochem. Photobiol. A Chem. 312 (2015) 55–63.
[24] A.E. Nogueira, E. Longo, E.R. Leite, E.R. Camargo, Synthesis and photocatalytic properties of bismuth titanate with different structures via oxidant peroxo method (OPM), J. Colloid Interface Sci. 415 (2014) 89–94.
[25] A.E. Nogueira, E. Longo, E.R. Leite, E.R. Camargo, Visible-light photocatalysis with bismuth titanate (Bi12TiO20) particles synthesized by the oxidant peroxide method (OPM), Ceram. Int. 41 (2015) 12073–12080.
[26] A.H. Pinto, F.L. Souza, A.J. Chiquito, E. Longo, E.R. Leite, E.R. Camargo, Characterization of dense lead lanthanum titanate ceramics prepared from powders synthesized by the oxidant peroxo method, Mater. Chem. Phys. 124 (2010) 1051–1056.
[27] A.H. Pinto, F.L. Souza, E. Longo, E.R. Leite, E.R. Camargo, Structural and dielectric characterization of praseodymium-modified lead titanate ceramics synthesized by the OPM route, Mater. Chem. Phys. 130 (2011) 259–263.
[28] J. Zou, J. Gao, F. Xie, An amorphous TiO2 sol sensitized with H2O2 with the enhancement of photocatalytic activity, J. Alloy. Comp. 497 (2010) 420–427.
[29] W.J. Shin, A.H. Granados, W.-H. Huang, H. Hu, M. Tao, Sulfurization of hematite Fe2O3 and anatase TiO2 by annealing in H2S, Mater. Chem. Phys. 222 (2019) 152–158.
[30] L. Aldon, P. Kubiak, M. Womes, J.C. Jumas, J. Olivier-Fourcade, J.L. Tirado, J.I. Corredor, C. Pérez Vicente, Chemical and electrochemical Li-insertion into the Li4Ti5O12 spinel, Chem. Mater. 16 (2004) 5721–5725.
[31] C.M. Julien, K. Zaghib, Electrochemistry and local structure of nano-sized Li4/3Me5/3O4 (MeMn, Ti) spinels, Electrochim. Acta 50 (2004) 411–416.
[32] D.G. Kellerman, V.S. Gorshkov, E.V. Shalaeva, B.A. Tsaryev, E.G. Vovkotrub, Structure peculiarities of carbon-coated lithium titanate: Raman spectroscopy and electron microscopic study, Solid State Sci. 14 (2012) 72–79.
[33] A.V. Knyazev, N.N. Smirnova, M. Mączka, S.S. Knyazeva, I.A. Letyanina, Thermodynamic and spectroscopic properties of spinel with the formula Li4/3Ti5/3O4, Thermochim. Acta 559 (2013) 40–45.
[34] I.A. Leonidov, O.N. Leonidova, L.A. Perelyaeva, R.F. Samigullina, S.A. Kovyazina, M.V. Patrakeev, Structure, ionic conduction, and phase transformations in lithium titanate Li4Ti5O12, Phys. Solid State 45 (2003) 2183–2188.
[35] E.V. Savinkina, L.N. Obolenskaya, G.M. Kuzmicheva, E.N. Kabachkov, A.A. Gainanova, Y.V. Zubavichus, V.Y. Murzin, N.V. Sadovskaya, Introduction of peroxo groups into titania: preparation, characterization and properties of the new peroxo-containing phase, CrystEngComm 17 (2015) 7113–7123.
[36] D. Xiao, G. He, Z. Sun, J. Lv, P. Jin, C. Zheng, M. Liu, Microstructure, optical and electrical properties of solution-derived peroxo-zirconium oxide gate dielectrics for CMOS application, Ceram. Int. 42 (2016) 759–766.
[37] A. Sivashanmugam, S. Gopukumar, R. Thirunakaran, C. Nithya, S. Prema, Novel Li4Ti5O12/Sn nano-composites as anode material for lithium ion batteries, Mater. Res. Bull. 46 (2011) 492–500.
[38] B. Vikram Babu, K. Vijaya Babu, G. Tewodros Aregai, L. Seeta Devi, B. Madhavi Latha, M. Sushma Reddi, K. Samatha, V. Veeraiah, Structural and electrical properties of Li4Ti5O12 anode material for lithium-ion batteries, Results Phys. 9 (2018) 284–289.